Combustion and Flame 160 (2013) 2434–2441

Contents lists available at SciVerse ScienceDirect

Combustion and Flame

journal homepage: www.elsevier.com/locate/combustflame

Measurement of the instantaneous flame front structure of syngas turbulent premixed flames at high pressure

Jinhua Wang [a,b,*], Meng Zhang [a], Zuohua Huang [a,*], Taku Kudo [b], Hideaki Kobayashi [b]

[a] State Key Laboratory of Multiphase Flow in Power Engineering, Xi'an Jiaotong University, Xi'an 710049, PR China
[b] Institute of Fluid Science, Tohoku University, Sendai, Miyagi 980-8577, Japan

ARTICLE INFO

Article history:
Received 24 December 2012
Received in revised form 4 April 2013
Accepted 6 June 2013
Available online 30 June 2013

Keywords:
Turbulent premixed flame
Syngas
Flame front
OH-PLIF
High pressure

ABSTRACT

Instantaneous flame front structure of syngas turbulent premixed flames including the local radius of curvature, the characteristic radius of curvature, the fractal inner cutoff scale and the local flame angle were derived from the experimental OH-PLIF images. The $CO/H_2/CO_2$/air flames as a model of syngas/air combustion were investigated at pressure of 0.5 MPa and compared to that of CH_4/air flames. The convex and concave structures of the flame front were detected and statistical analysis including the PDF and ADF of the local radius of curvature and local flame angle were conducted. Results show that the flame front of turbulent premixed flames at high pressure is a wrinkled flame front with small scale convex and concave structures superimposed with large scale flame branches. The convex structures are much more frequent than the concave ones on flame front which reflects a general characteristic of the turbulent premixed flames at high pressure. The syngas flames possess much wrinkled flame front with much smaller fine cusps structure compared to that of CH_4/air flames and the main difference is on the convex structure. The effect of turbulence on the general wrinkled scale of flame front is much weaker than that of the smallest wrinkled scale. The general wrinkled scale is mainly dominated by the turbulence vortex scale, while, the smallest wrinkled scale is strongly affected by the flame intrinsic instability. The effect of flame intrinsic instability on flame front of turbulent premixed flame is mainly on the formation of a large number of convex structure propagating to the unburned reactants and enlarge the effective contact surface between flame front and unburned reactants.

1. Introduction

Integrated Gasification Combined Cycle (IGCC) technology has attracted increasing attention in recent years due to its superior advantages such as fuel diversity and suitability for Carbon Capture and Storage (CCS) [1,2]. For IGCC, not only coal, but the low grade fuel like heavy oil, petroleum coke, biomass and waste can also be used by gasification. IGCC can realize zero CO_2 emissions when it is extended to CCS [3]. For IGCC power plant, the coal or other fuel resources are gasified and the derived gas is called syngas with the main composition of CO and H_2 [4]. Compared to typical hydrocarbons, syngas has higher laminar burning velocity, higher mass diffusivity and thus lower Lewis number. Consequently, the turbulence–chemistry interaction for turbulent premixed flames of syngas/air mixtures would be significantly different from that of typical hydrocarbon/air mixtures in modern premixed-type gas turbine. Thus in addition to the extensive studies on turbulent hydrocarbon/air flames, there has been growing interest in turbulent syngas/air flames. Specifically, the turbulent burning velocity of sygnas has been measured over a wide range of fuel composition, dilution and turbulence conditions. The interaction between turbulence and flame was discussed in detail based on the length and time scale of turbulence and chemical reaction, considering the stretch sensitivity and diffusivity of the reactants [5–7]. Our previous researches of the experimental study of syngas/air turbulent premixed flames at high pressure showed that syngas/air flame possess many fine cusps in the flame front compared to that of CH_4/air flame, and these small cusps being superimposed on the large scale wrinkled flame front even for low turbulence condition [8,9]. Additionally, the flame volume derived from the OH-PLIF images indicated that the flame volume of syngas/air flames are much smaller than that of CH_4/air flames, which will potentially result in a higher possibility to cause combustion oscillation in premixed-type gas turbine combustors [10]. However, the detail flame front characteristics were still not well investigated in quantitative.

Flame front structure reveals the interaction between turbulence and flame, and it can also be used for turbulent combustion modeling. Up to now, a complete geometric description of

* Corresponding authors. Address: State Key Laboratory of Multiphase Flow in Power Engineering, Xi'an Jiaotong University, Xi'an 710049, PR China (J. Wang). Fax: +86 29 82668789.
E-mail addresses: jinhuawang@mail.xjtu.edu.cn (J. Wang), zhhuang@mail.xjtu.edu.cn (Z. Huang).

0010-2180/$ - see front matter © 2013 The Combustion Institute. Published by Elsevier Inc. All rights reserved.
http://dx.doi.org/10.1016/j.combustflame.2013.06.008

turbulent premixed flame front has been provided, such as fractal dimension and cutoff scales [11–13], flame curvature and angle statistics [14,15]. The effects of Lewis number [15,16], pressure [17–19] and turbulence intensity on flame front structure have been studied. However, few studies were reported on the syngas flames, especially under high pressure conditions mainly due to experimental difficulty. Flame curvature and its statistical properties such as PDF (probability density function) are usually used to indicate the wrinkled flame front structure. However, it cannot properly indicate the small scale structure on the flame front because the small scale structure with large curvature are located far from the center and may even fall out of the figure of the PDF of curvature [14,15,18]. This behavior will be even more obvious for syngas flames at high pressure as our previous studies showed that syngas flames possess much finer structure with smaller scale compared to that of CH_4/air flames [8], and turbulent premixed flames at high pressure possess a much finer wrinkled structure with a much smaller scale of convex and concave structure compared with that at ordinary pressure [9,19,20]. Thus, the detailed small scale flame front structure of syngas turbulent premixed flames at high pressure is very important and needs further study. The local radius of curvature of flame front can be treated as a length scale [21], and it is used in the present study with a focus on the small scale convex and concave structure on flame front.

The objective of the present study is to explore the instantaneous flame front characteristics of syngas turbulent premixed flames at high pressure. $CO/H_2/CO_2$/air mixtures as a model of syngas/air combustion were investigated and compared to that of CH_4/air flames. A series of complete geometric parameters including the local radius of curvature, the fractal inner cutoff scale and the local flame angle were obtained and the statistical analysis was conducted. Interaction between turbulence and flame were examined based on the statistical analysis and the length scales of turbulence, laminar flames and turbulent premixed flames.

2. Experimental setup and procedures

Experiments were performed using the high-pressure combustion test facility at the Institute of Fluid Science, Tohoku University [22]. A brass nozzle-type burner with an outlet diameter of 20 mm was used. Turbulence was generated by a perforated plate installed 40 mm upstream of the outlet. Four perforated plates with different hole diameter and opening ratio combined with mean jet velocity were used to generate different turbulence condition. Turbulence measurement at high pressure was conducted using a constant-temperature hot-wire anemometer (Dantec, Streamline 90N). Bunsen-type turbulent premixed flames of $CO/H_2/CO_2$/air mixtures and/or CH_4/air mixtures were stabilized at the nozzle burner outlet in the high-pressure chamber as shown in Fig. 1. A large amount of fresh air was supplied to the chamber to keep the pressure constant at 0.5 MPa and to prevent the chamber from filling with burned gases. Fuel and air were premixed and supplied to the burner at temperature of 300 K. More details of the experimental facility and turbulence measurement have been described elsewhere [20,23].

Table 1
Properties of the mixtures in this study.

Mixtures	P (MPa)	ϕ	S_L (cm/s)	T_{ad} (K)	δ (mm)	Le_{eff}	L_M (mm)	li (mm)
$CO/H_2/CO_2$/air	0.5	0.7	18.4	1888	0.029	0.605	0.072	0.350
CH_4/air	0.5	1.0	18.8	2253	0.024	1.048	0.1	0.666

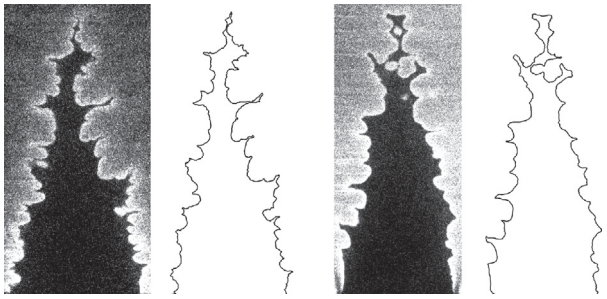

Fig. 2. OH-PLIF images and the binarization curve. ($u'/S_L \cong 0.55$).

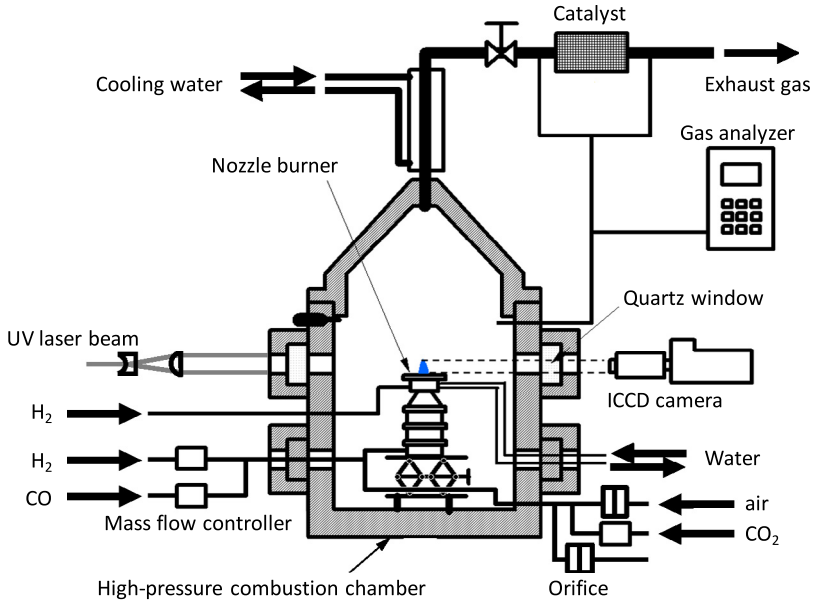

Fig. 1. Schematic of the high-pressure combustion facility [22].

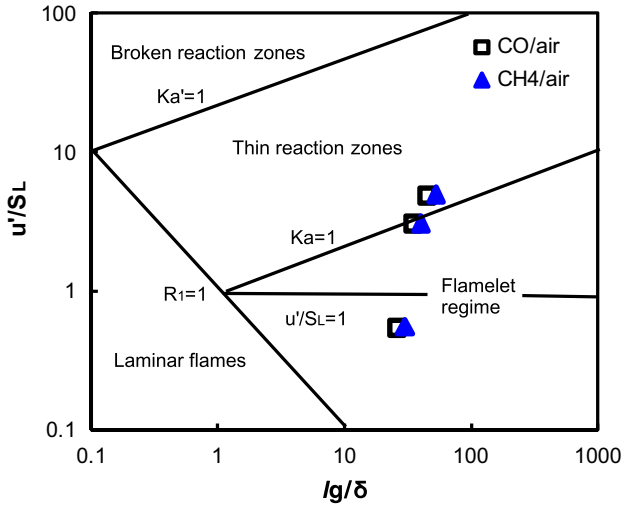

Fig. 3. Borghi's diagram of turbulent premixed flames revised by Peters [32]. lg is integral scale and δ is laminar flame thickness.

For the $CO/H_2/CO_2$/air mixtures in this study, the $XCO/XH_2 = 65/35$ and $XCO_2/(XCO + XH_2 + XCO_2) = 0.3$ represent the model syngas composition [8], X means the mole fraction of the specific species. The properties of the mixtures are summarized in Table 1. Laminar burning velocity, S_L, was calculated using the PREMIX code [24] and CHEMKIN-II database [25] with the mechanism of Frassoldati et al. [26] for $CO/H_2/CO_2$/air mixture and GRI-Mech 2.11 [27] for CH_4/air mixture. Effective Lewis number, Le_{eff}, was calculated using the equation, $1/Le_{eff} = (X_1/Le_1 + X_2/Le_2 + \cdots + X_i/Le_i)/(X_1 + X_2 + \cdots X_i)$, where X_i and Le_i are the mole fraction and Lewis number of considered species i [28]. This equation is based on diffusion coefficient of multi-component fuel and oxidizer considering stoichiometry. Thus, for lean $CO/H_2/CO_2$/air mixture, the species considered were CO and H_2. For the stochiometric CH_4/air mixtures, the species considered were CH_4 and O_2. Adiabatic flame temperature, T_{ad}, laminar flame thickness, δ, Markstein length, L_M [29], and flame intrinsic instability scale, l_i [30], were also calculated and given in Table 1. Laminar flame thickness, δ, is dtermined as [31],

$$\delta = \frac{D_{th}}{S_L} \tag{1}$$

where D_{th} is the thermal diffusivity of unburned gas, which is defined as

$$D_{th} = \frac{\lambda}{\rho C_p} \tag{2}$$

where λ, ρ and C_p are the thermal conductivity, density and specific heat of unburned gas, respectively.

OH-PLIF measurements were performed to visualize the instantaneous flame front. An Nd-YAG laser (Spectra Physics, GCR-250-10) and a dye laser with a frequency doubler (Spectron, SL4000) were used. The wavelength of 532 nm from the YAG laser was used, and the laser sheet with wavelength of 282.929 nm from the frequency doubler was used for OH radical excitation. A blended branch of $Q_1(9)$ and $Q_2(8)$ for (1,0) bands of the OH radical was selected for the OH excitation, and almost all OH-LIF emission from the (0,0) band with 308 nm was detected using a high resolution ICCD camera (ANDOR, DH574-18F) with UV lens (Nikkon, UV-105 mm, F4.5s), a low-pass filter (WG-295), and a broad band-pass filter (UG-5). Thickness of the laser sheet was less than 50 μm and the laser height was about 50 mm at the flame position, and the maximum energy of a single laser shot was about 11 mJ. The OH-PLIF image is 1024 × 1024 pixels and the finest pixel resolution is 0.054 mm/pixel at the measurement plane.

The flame front structure was derived from the OH-PLIF image by binarizing with a threshold value based on histogram of the

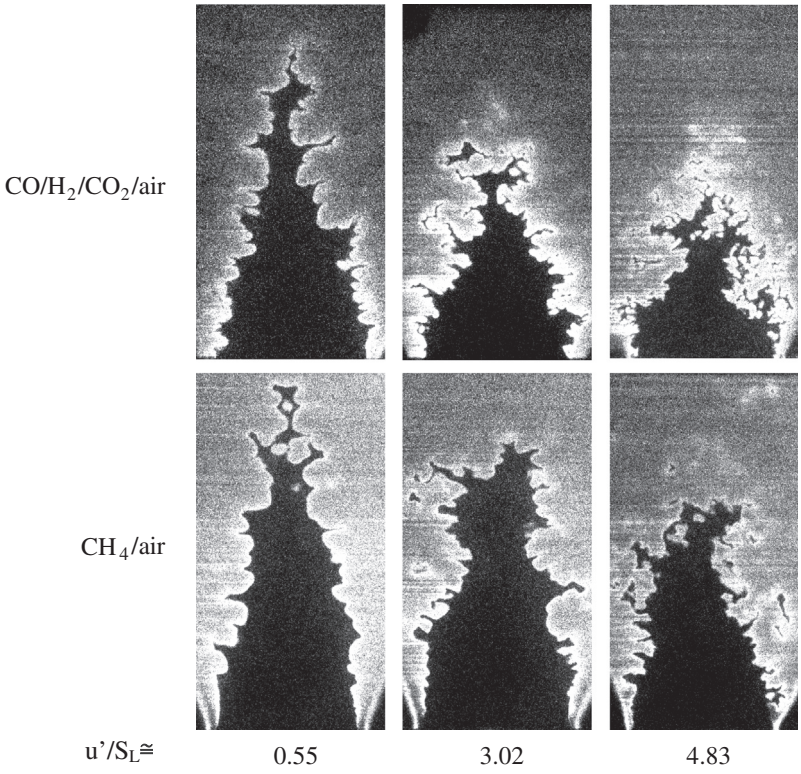

Fig. 4. OH-PLIF images of the turbulent premixed flames under various turbulence conditions.

intensity of the images. Flame front was tracked as shown in Fig. 2. It shows that the strongly convoluted flame front can be well recognized at the binarization curve by using the high resolution and high sensitivity OH-PLIF technique in this study. Thus it is used for the calculation of flame front structure. A third order smoothing scheme was used to remove the digitization noise of the binarization process. The smooth flame surface was then discretized with an interval of 0.31 mm which was the smallest inner cutoff scale of all flames in this study. The use of this interval and discretization is to remove the digitization noise from the pixel [15] since the inner cutoff scale can be viewed as the smallest scale of the flame front. The discretized points were fitted using a 3-order spline interpolation scheme, which was then employed to calculate the local radius of curvature, R, and local flame angle, α, through the following equations:

$$R = \frac{(x(s)'^2 + y(s)'^2)^{3/2}}{x(s)'y(s)'' - y(s)'x(s)''} \tag{3}$$

$$\alpha = \arctan(y(s)'/x(s)') \tag{4}$$

where $x(s)$ and $y(s)$ are coordinates of the flame front spline curve and s is the length of the accumulated flame from the starting point. For the local radius of curvature, the positive direction was defined as being convex to the unburned mixture. The local flame angle was defined from the flame front normal vector to the upward vertical axis in a counterclockwise direction. The fractal inner cutoff scale, ε_i, was calculated by using 50 OH-PLIF images with the circle method [23].

A total of 60 images were calculated for each condition and statistical analysis of the local radius of curvature and local flame angle was conducted including the PDF and ADF (accumulated distribution function) distributions as follows:

$$ADF(R) = \int_0^R PDF\, dR \tag{5}$$

The range for the calculation of the radius of curvature is from −100 to 100 mm. The interval for PDF calculation is 0.02 mm for the radius of curvature, and 6° for the local flame angle, respectively.

3. Results and discussions

3.1. Length scale characteristics of flame front structure

The Borghi's diagram of turbulent premixed flames revised by Peters [32] is shown in Fig. 3. It shows that most of the flames in this study are located in the indicating flamelet regime; thus the flame characteristics can be discussed by assuming flamelet regime. The OH-PLIF images of the $CO/H_2/CO_2$/air mixtures and CH_4/air mixtures under various u'/S_L are shown in Fig. 4. It shows that all flames in this study possess fine and convoluted flame front structure which is a general characteristic of the turbulent premixed flames at high pressure [20]. The flame front of $CO/H_2/CO_2$/air flames are much finer and wrinkled compared to that of CH_4/air flame. The $CO/H_2/CO_2$/air flames have a large number of fine cusps and these fine cusps with small scale are superimposed on large-scale convex and concave flame wrinkles. While, in the case of CH_4/air flame, large scale and deep flame branches without fine scale cusps are formed leading to a thicker turbulent flame brush and larger flame volume [8]. Small scale sharp concave structures propagating to the burned mixture and large scale convex structures propagating to the unburned mixture are much more frequent on flame front for all conditions. With the increase of u'/S_L, flame height tends to be lower and flame front tends to be finer due to the decrease of turbulence scale which wrinkle the flame front. This is a general observation from the OH-PLIF images. In the following, quantitative analysis of the flame front structure will be presented to interpret the above experimental observation and turbulence–flame interaction.

Figure 5 shows the PDF and ADF distributions of the local radius of curvature. As shown in Fig. 5a, the PDF of the radius of curvature shows an obvious bias to positive radius corresponding to the convex structure. The convex structure becomes much more frequent for $CO/H_2/CO_2$/air flames compared to CH_4/air flames, while the frequency of the concave structure shows no obvious difference. The peak of the PDF for $CO/H_2/CO_2$/air flames is much larger than that of CH_4/air flames suggests that the small scale structure is much more frequent for $CO/H_2/CO_2$/air flames. The ADF in Fig. 5b shows the whole calculated range of the local radius of curvature. Similar tendency with PDF distribution was observed. In the following section, the local radius of curvature at a small scale range of −5 to 5 mm is used to discuss the small scale structure in details.

The ADF of the radius of curvature for syngas/air flames and CH_4/air flames under various conditions are given in Fig. 6. The radius of curvature with positive value is always more than that of the negative ones under all conditions in this study. This indicates that the convex structure, which is convex to the unburned mixtures, is always more frequent than that of the concave structure for turbulent premixed flame. This is a general characteristic of

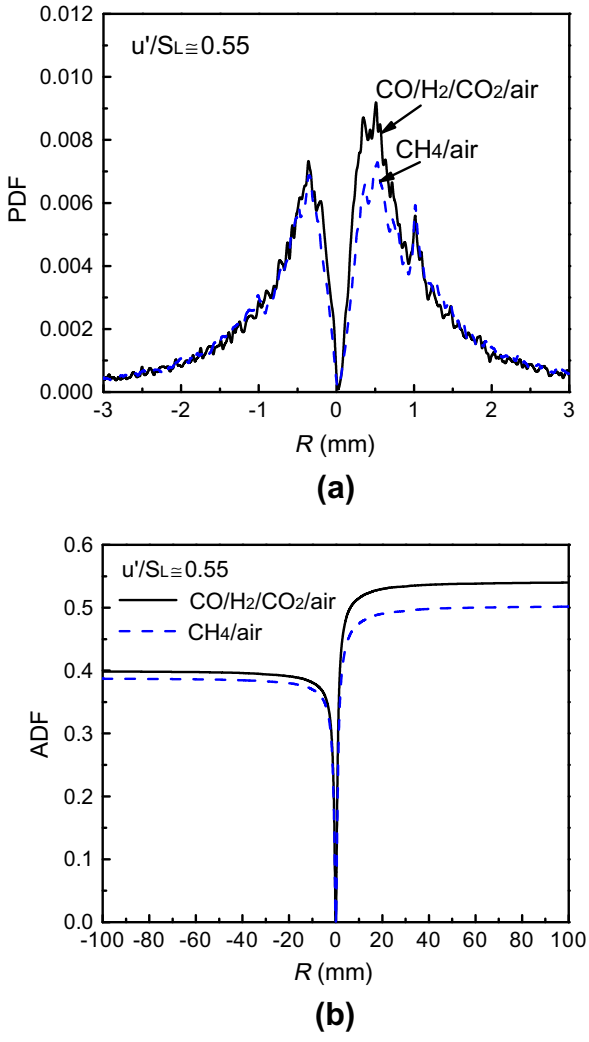

Fig. 5. PDF and ADF distributions of the local radius of curvature: (a) PDF distribution; (b) ADF distribution.

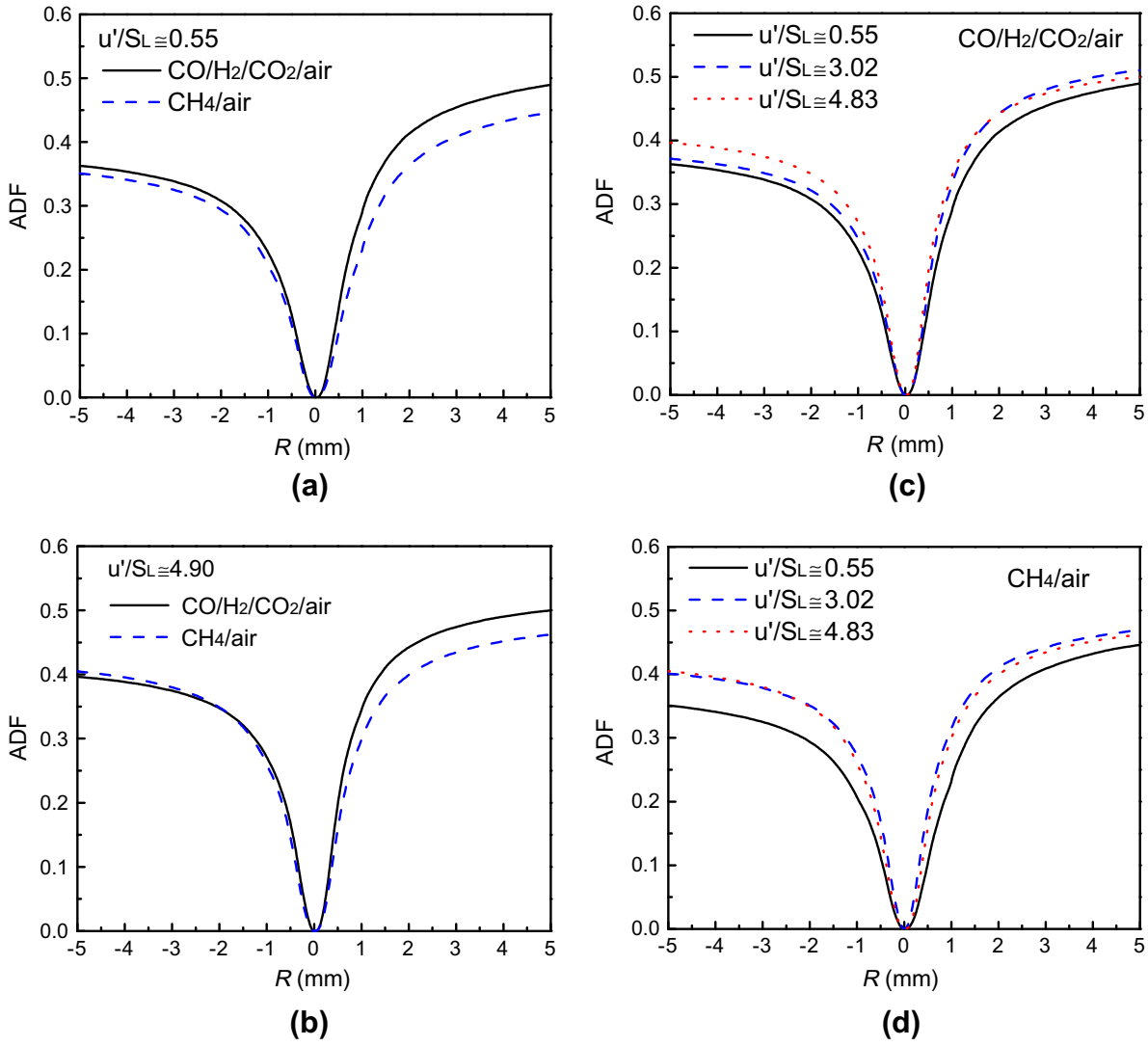

Fig. 6. The ADF of radius of curvature: (a) $u'/S_L \cong 0.55$; (b) $u'/S_L \cong 4.9$; (c) $CO/H_2/CO_2$/air flames; (d) CH_4/air flames.

the turbulent premixed flame at high pressure. This phenomenon can also be observed from the OH-PLIF images as shown in Fig. 4 and is consistent with the observation of Kobayashi et al. [20] and now it was validated from the quantitative flame front structure analysis. Previous researches using the PDF of curvature to indicate the flame front structure generally showed a nearly symmetrical distribution with a mean of approximately zero [15,17,18,33–35] although some studies found a slightly positive bias which was convex to the unburned mixture [14,19,36]. Up to now, there is no consensus as to the distribution of local flame curvature and the local flame curvature on the overall burning rate is still not well understood. This may be due to the fact that the flat pattern on the flame front with a small curvature which is near zero locates at the center of the PDF of curvature, while the small scale structure has a large local curvature which is far from the center and may even be out of the range of previous researches [14,15,19]. Thus, the small scale structure with large curvature was not properly presented by using the PDF of curvature in previous researches. This problem is even more severe for syngas flames at high pressure as flame front is more wrinkled with a much smaller scale structure corresponding to a much larger curvature. By using the local radius of curvature in this study, the small scale structure and its distribution can be well presented and a higher probability of positive structure which is convex to unburned mixtures is clearly indicated.

Results also show that most of the radius of curvature of flame front locate at small scale range with small scale structure. This indicates that the flame front of turbulent premixed flame is wrinkled flame front with small scale structure as shown in Fig. 4. Figure 6 shows that the radius of curvature is affected by the mixtures and turbulence intensity. As shown in Fig. 6a and b that the radius of curvature tends to be smaller for $CO/H_2/CO_2$/air flames compared to CH_4/air flames. This difference is more obvious at convex structure. This would be due to the lower effective Lewis number and Markstein length of $CO/H_2/CO_2$/air mixtures, leading to the passivity response of flame to turbulence. Figure 6c and d shows the effect of turbulence intensity on the ADF of radius of curvature. Both the ADF of convex and concave structure increase with the increase of turbulence intensity. This indicates that the quantity of the small scale structure on flame front increase with the increase of turbulence intensity. This effect is more obvious at low turbulence intensity, while the effect becomes weakly at middle and high intensity. This indicates that the increase of S_T/S_L with the increase of u'/S_L is due to the increase of the quantity of the structure on flame front

in flamelet regime. This is consistent to our previous study that the increase of S_T/S_L with the increase of u'/S_L is more significantly under weak turbulence intensity condition [37].

The characteristic radius of curvature, $R_{0.5}$, which is a characteristic length scale of the wrinkled flame front, is defined as the absolute local radius of curvature at ADF = 0.5 as shown in Fig. 7a. Here only the magnitude is considered regardless of direction. This means that 50% of the wrinkled structure is located at a scale smaller than $R_{0.5}$, and it is regarded as the average radius of curvature on flame front. The length scale of turbulence (mean diameter of vortex in isotropic turbulence, l_v, is about $10\eta_k$ as reported by Tanahashi et al. [38], where η_k is Kolmogorove scale), laminar flame (the intrinsic flame instability, l_i, indicates the combined effect of hydrodynamic instability and diffusive-thermal instability, corresponds to the wavelength at the maximum growth rate of flame front disturbance calculated using Sivashinsky's formulation [30]), and turbulent premixed flame (fractal inner cutoff scale, ε_i, and characteristic radius of curvature, $R_{0.5}$) are given in Fig. 7b. Both ε_i and $R_{0.5}$ are the characteristic scales of the wrinkled flame front of turbulent premixed flames. However, the physical meanings are quite different. ε_i represents the smallest scale corresponding to the smallest wrinkled structure on flame front, while $R_{0.5}$ refers to the average scale of the flame front wrinkled structure and reflects the general wrinkled level of the flame front. Both ε_i and $R_{0.5}$ decrease with the increase of u'/S_L mainly caused by the small scale turbulence interaction as turbulence scale, l_v, decreases with the increase of u'/S_L. Both ε_i and $R_{0.5}$ are smaller for $CO/H_2/CO_2$/air flames compared to CH_4/air flames under the same turbulence condition. This is due to the intrinsic instability of the laminar flame that affects the response of the laminar flame to turbulence. It is seen that the intrinsic instability scale of $CO/H_2/CO_2$/air flame is l_i = 0.35 mm, which is much smaller than that of CH_4/air flame (l_i = 0.66 mm). It is noted that the decrease of ε_i is more obvious compared to $R_{0.5}$ with the increase of u'/S_L, and this reflects the finer and sharper small scale structure. However, the overall wrinkled scale decreases slightly with the increase of u'/S_L, and this indicates that the general wrinkled scale of the flame front is mainly determined by the turbulence vortex scale, while, the smallest wrinkled scale is mainly affected by the flame intrinsic instability. The lower limit of the smallest wrinkled scale is the flame intrinsic instability scale as reported by our previous research [13,23].

Percentage of the convex and concave structure is given in Fig. 8a. The data above the dot line is positive corresponding to

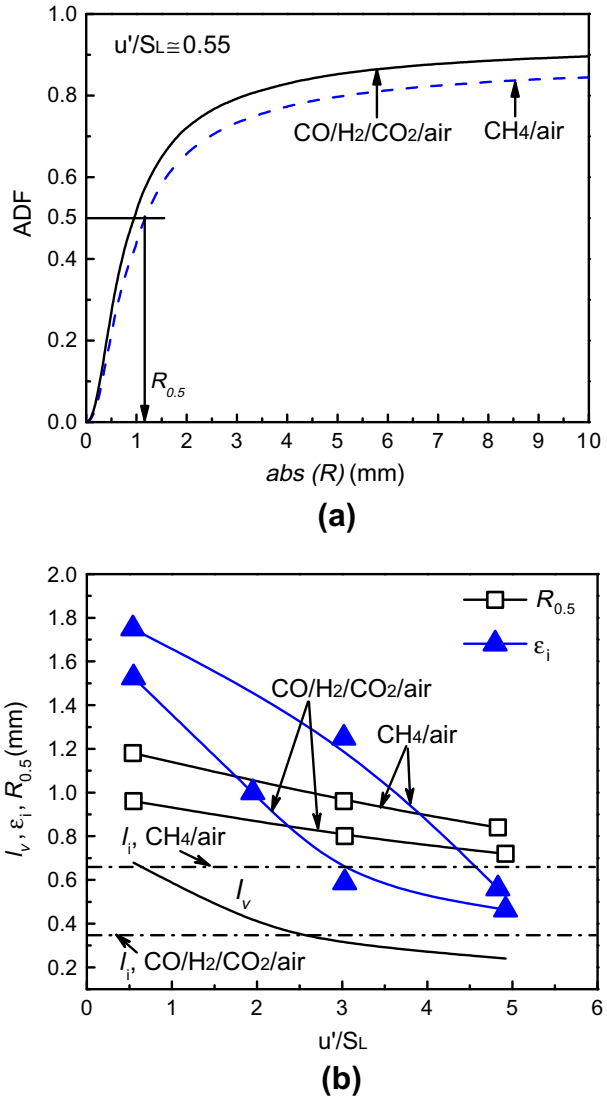

Fig. 7. Determination of $R_{0.5}$, variation of characteristic length scales of turbulent flame and flow turbulence with u'/S_L: (a) definition of $R_{0.5}$; (b) $R_{0.5}$, l_i, ε_i and l_v.

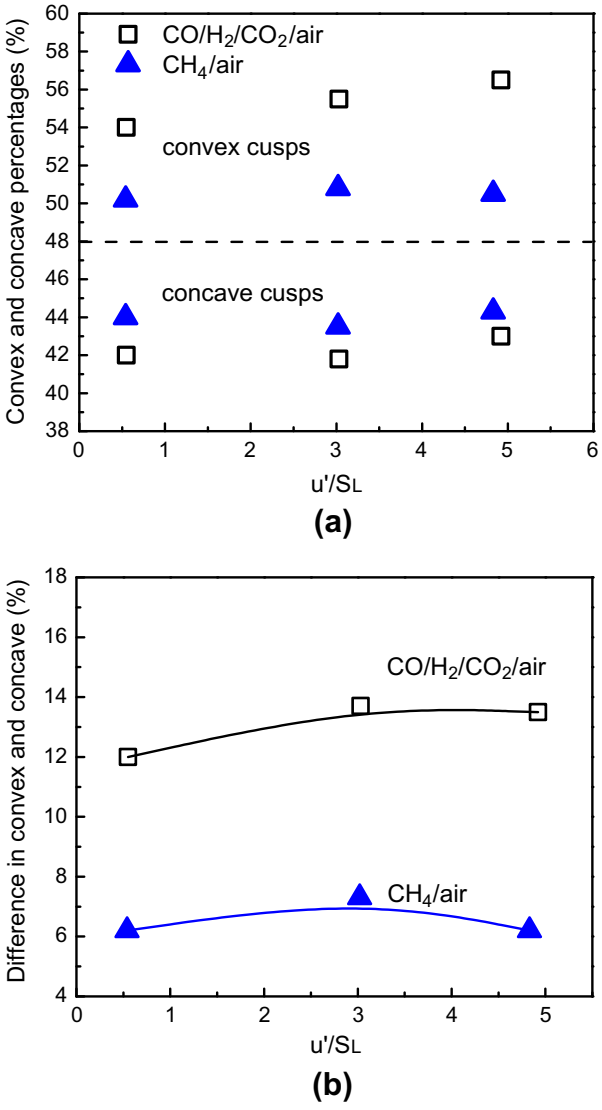

Fig. 8. Variations of convex and concave percentages on flame front with u'/S_L: (a) convex and concave percentages; (b) difference in convex and concave percentages.

the convex structure and that below the dot line is the concave structure. Besides the convex and concave structure in the flame front, there are also flat patterns. The radius of curvature is infinity for these flat patterns and out of the range of the calculation, i.e., −100 to 100 mm, thus, the total ADF is always less than unity. It can be seen from Fig. 8a that there are about 1–6% flat patterns for all the conditions in this study. Percentage of concave structure shows little difference for all flames in this study while there is a big difference between $CO/H_2/CO_2$/air flames and CH_4/air flames for the convex structure. This suggests that the generation of much fine and wrinkled structure on flame front for $CO/H_2/CO_2$/air flames is due to the formation of a large numbers of convex structure on flame front. The formation and movement of the convex structure on flame front penetrates into the unburned mixtures and increases the effective contact surface between flame front and unburned reactant. This is one of the mechanisms to cause the fine wrinkled structure at high pressure. This also leads to the result that the S_T/S_L of $CO/H_2/CO_2$/air flames is larger than that of CH_4/air flames as reported in our previous researches [8,9].

Difference in percentage of convex and concave structure is given in Fig. 8b. The difference between convex and concave structure for $CO/H_2/CO_2$/air flames is much larger than that of CH_4/air flames. As discussed previously, it will be one of the mechanisms to generate fine and wrinkled structures on flame front. The difference between $CO/H_2/CO_2$/air flames and CH_4/air flames on convex and concave structure is supposed to be closely related to the interaction between flame front and turbulence vortex. Since the turbulence characteristics for the two flames at the same u'/S_L is almost the same, the difference should be due to the flame intrinsic instability which leads to the different response of flame to turbulence. As shown in Table 1, the effective Lewis number of $CO/H_2/CO_2$/air flames is 0.605 and much less than 1.0 while that of CH_4/air is nearly unity. The flame intrinsic instability scale, l_i, of $CO/H_2/CO_2$/air flame is much smaller than that of CH_4/air flame as shown in Fig. 7b. The flame intrinsic instability of $CO/H_2/CO_2$/air flames leads to the formation of much fine and wrinkled structure on flame front and the effect is mainly on the formation of convex structure.

3.2. Orientation characteristics of the flame front structure

Local flame angle reflects the distribution of flame front normal vectors and is an important flame front geometric property which is potentially applicable in turbulent flame modeling [39]. As defined above, the local flame angle is measured from the flame front normal vector to the upward vertical axis in the counter-clockwise direction as shown in Fig. 9. Positive value indicates that the flame front is concave to the unburned mixture and that the larger angle corresponds to the flamelet propagating upward. The PDF distribution of the local flame angle is given in Fig. 9. It shows that the PDF distribution of local flame angle for $CO/H_2/CO_2$/air flames and CH_4/air flames are similar with their peak position at about 120°. The $CO/H_2/CO_2$/air flames shows relatively higher probability at 120° and this indicated that the local flame tends to propagate upward and that the most frequent structure is the concave structure propagating upward.

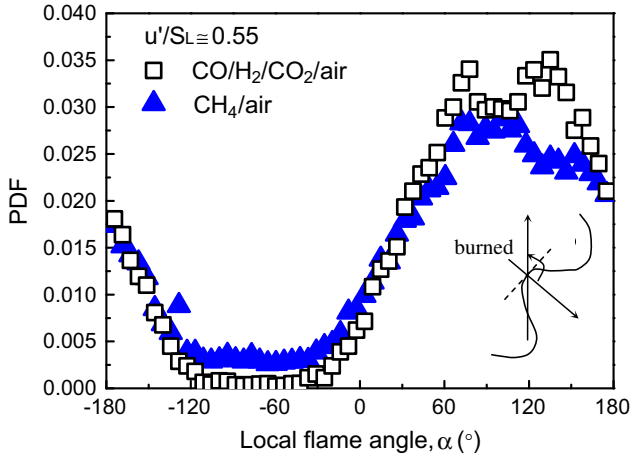

Fig. 9. PDF distribution of the local flame angle.

4. Conclusions

The instantaneous detailed flame front structure of turbulent premixed flames for $CO/H_2/CO_2$/air mixtures as a model of syngas/air combustion at high pressure were measured and compared with that of CH_4/air flames. A series of complete geometric parameters were derived from the experimental OH-PLIF images, including the local radius of curvature, the characteristic radius of curvature, the fractal inner cutoff scale and the local flame angle. Interaction between turbulence vortex and flame was discussed based on the above parameters combined with the length scales of laminar flame and turbulence. Main results are summerized as follows:

1. The flame front of turbulent premixed flames at high pressure is a wrinkled flame front with small scale convex and concave structures superimposed with large scale flame branches. Convex structures are much more frequent than the concave ones of the flame front and we have the strong indication that this is a general characteristic of the turbulent premixed flames at high pressure.
2. Syngas flames possess much wrinkled flame front with much smaller fine cusps structure compared to that of CH_4/air flame. Main difference is on their convex structure from the quantitative flame front structure analysis.
3. Effect of turbulence on general wrinkled scale of flame front is much weaker than that of the smallest wrinkled scale. The general wrinkled scale is mainly dominated by turbulence vortex scale, while, the smallest wrinkled scale is mainly determined by flame intrinsic instability.
4. Effect of the flame intrinsic instability on flame front of turbulent premixed flame is reflected by the formation of a large numbers of convex structure which propagate to the unburned reactants and enlarge the effective contact surface between flame front and unburned reactants.

Acknowledgments

This study is partially supported by National Natural Science Foundation of China (No. 51006080) and the Fundamental Research Funds for the Central Universities. Authors express their thanks to Prof. Yasuhiro Ogami, Dr. Masaki Okuyama and Mr. Futoshi Matsuno at Tohoku University for their helpful and stimulating discussion. Jinhua Wang acknowledges the Japan Society for the Promotion of Science for a JSPS postdoctoral Fellowship grant.

References

[1] J.P. Longwell, E.S. Rubin, J. Wilson, Prog. Energy Combust. Sci. 21 (1995) 269–360.
[2] T.F. Wall, Proc. Combust. Inst. 31 (2007) 31–47.
[3] B.J.P. Buhre, L.K. Elliott, C.D. Sheng, R.P. Gupta, T.F. Wall, Prog. Energy Combust. Sci. 31 (2005) 283–307.

[4] J. Natarajan, Y. Kochar, T. Lieuwen, J. Seitzman, Proc. Combust. Inst. 32 (2009) 1261–1268.
[5] P. Venkateswaran, A. Marshall, D.H. Shin, D. Noble, J. Seitzman, T. Lieuwen, Combust. Flame 158 (2011) 1602–1614.
[6] C.C. Liu, S.S. Shy, C.W. Chiu, M.W. Peng, H.J. Chung, Int. J. Hydrogen Energy 36 (2011) 8595–8603.
[7] P. Venkateswaran, A. Marshall, J. Seitzman, T. Lieuwen, Proc. Combust. Inst. 34 (2013) 1527–1535.
[8] Y. Ichikawa, Y. Otawara, H. Kobayashi, Y. Ogami, T. Kudo, M. Okuyama, S. Kadowaki, Proc. Combust. Inst. 33 (2011) 1543–1550.
[9] H. Kobayashi, Y. Otawara, J. Wang, F. Matsuno, Y. Ogami, M. Okuyama, T. Kudo, S. Kadowaki, Proc. Combust. Inst. 34 (2013) 1437–1445.
[10] S. Kato, T. Fujimori, A.P. Dowling, H. Kobayashi, Proc. Combust. Inst. 30 (2005) 1799–1806.
[11] G.J. Smallwood, Ö.L. Gülder, D.R. Snelling, B.M. Deschamps, I. Gökalp, Combust. Flame 101 (1995) 461–470.
[12] Ö.L. Gülder, G.J. Smallwood, R. Wong, D.R. Snelling, R. Smith, B.M. Deschamps, J.C. Sautet, Combust. Flame 120 (2000) 407–416.
[13] H. Kobayashi, H. Kawazoe, Proc. Combust. Inst. 28 (2000) 375–382.
[14] I.G. Shepherd, W.T. Ashurst, Proc. Combust. Inst. 24 (1992) 485–491.
[15] T.W. Lee, G.L. North, D.A. Santavicca, Combust. Flame 93 (1993) 445–456.
[16] C.J. Rutland, A. Trouvé, Combust. Flame 94 (1993) 41–57.
[17] A. Soika, F. Dinkelacker, A. Leipertz, Combust. Flame 132 (2003) 451–462.
[18] T. Lachaux, F. Halter, C. Chauveau, I. Gökalp, I.G. Shepherd, Proc. Combust. Inst. 30 (2005) 819–826.
[19] C. Cohe, F. Halter, C. Chauveau, I. Gokalp, O.L. Gulder, Proc. Combust. Inst. 31 (2007) 1345–1352.
[20] H. Kobayashi, T. Nakashima, T. Tamura, K. Maruta, T. Niioka, Combust. Flame 108 (1997) 104–110.
[21] J. Wang, F. Matsuno, M. Okuyama, Y. Ogami, H. Kobayashi, Z. Huang, Proc. Combust. Inst. 34 (2013) 1429–1436.
[22] H. Kobayashi, Exp. Thermal Fluid Sci. 26 (2002) 375–387.
[23] H. Kobayashi, T. Kawahata, K. Seyama, T. Fujimari, J.-S. Kim, Proc. Combust. Inst. 29 (2002) 1793–1800.
[24] R.J. Kee, F.M. Rupley, J.A. Miller, Report SAND89-8009B, Sandia National Laboratories, Albuquerque, NM, 1993.
[25] R.J. Kee, J.F. Grcar, M.D. Smooke, J.A. Miller, Report SAND85-8240, Sandia National Laboratories, Albuquerque, NM, 1985.
[26] A. Frassoldati, T. Faravelli, E. Ranzi, Int. J. Hydrogen Energy 32 (2007) 3471–3485.
[27] C.T. Bowman, R.K. Hanson, D.F. Davidson, W.C. Gardiner, V. Lissianski Jr., G.P. Smith, D.M. Golden, M. Frenklach, M. Goldenberg, 1994.
[28] F. Dinkelacker, B. Manickam, S.P.R. Muppala, Combust. Flame 158 (2011) 1742–1749.
[29] M.J. Brown, I.C. McLean, D.B. Smith, S.C. Taylor, Proc. Combust. Inst. 26 (1996) 875–881.
[30] J. Yuan, Y. Ju, C.K. Law, Proc. Combust. Inst. 31 (2007) 1267–1274.
[31] C.K. Law, C.J. Sung, Prog. Energy Combust. Sci. 26 (2000) 459–505.
[32] N. Peters, Turbulent Combustion, Cambridge University Press, Cambridge, UK, 2000.
[33] M.Z. Haq, C.G.W. Sheppard, R. Woolley, D.A. Greenhalgh, R.D. Lockett, Combust. Flame 131 (2002) 1–15.
[34] D. Bradley, P.H. Gaskell, A. Sedaghat, X.J. Gu, Combust. Flame 135 (2003) 503–523.
[35] F.T.C. Yuen, Ö.L. Gülder, Proc. Combust. Inst. 32 (2009) 1747–1754.
[36] K.N.C. Bray, R.S. Cant, Proc. R. Soc. Lond. A 434 (1991) 217–240.
[37] H. Kobayashi, K. Seyama, H. Hagiwara, Y. Ogami, Proc. Combust. Inst. 30 (2005) 827–834.
[38] M. Tanahashi, S.J. Kang, T. Miyamoto, S. Shiokawa, T. Miyauchi, Int. J. Heat Fluid Flow 25 (2004) 331–340.
[39] T.C. Chew, K.N.C. Bray, R.E. Britter, Combust. Flame 80 (1990) 65–82.